Review

Enlightening molecular mechanisms through study of protein interactions

Josep Rizo*, Michael K. Rosen, and Kevin H. Gardner

Departments of Biophysics, Biochemistry and Pharmacology, University of Texas Southwestern Medical Center, 6000 Harry Hines Boulevard, Dallas, TX 75390, USA
* Correspondence to: Josep Rizo, E-mail: jose@arnie.swmed.edu

The investigation of molecular mechanisms is a fascinating area of current biological research that unites efforts from scientists with very diverse expertise. This review provides a perspective on the characterization of protein interactions as a central aspect of this research. We discuss case studies on the neurotransmitter release machinery that illustrate a variety of principles and emphasize the power of combining nuclear magnetic resonance (NMR) spectroscopy with other biophysical techniques, particularly X-ray crystallography. These studies have shown that: (i) the soluble SNAP receptor (SNARE) proteins form a tight complex that brings the synaptic vesicle and plasma membranes together, which is key for membrane fusion; (ii) the SNARE syntaxin-1 adopts an autoinhibitory closed conformation; (iii) Munc18-1 plays crucial functions through interactions with closed syntaxin-1 and with the SNARE complex; (iv) Munc13s mediate the opening of syntaxin-1; (v) complexins play dual roles through distinct interactions with the SNARE complex; (vi) synaptotagmin-1 acts a Ca^{2+} sensor, interacting simultaneously with the membranes and the SNAREs; and (vii) a Munc13 homodimer to Munc13-RIM heterodimer switch modulates neurotransmitter release. Overall, this research underlines the complexities involved in elucidating molecular mechanisms and how these mechanisms can depend critically on an interplay between strong and weak protein interactions.

Keywords: molecular mechanisms, protein interactions, NMR spectroscopy, neurotransmitter release, membrane fusion, X-ray crystallography

Introduction

Life depends on an immense variety of biological processes that are often controlled by complex protein machineries. Major efforts are dedicated to study the molecular mechanisms underlying how these machineries function, both because of the fundamental value of such knowledge and because it can guide the design of therapies for diseases that arise from defects in these systems. Key aspects of these investigations are the discovery of proteins that govern the process, the analysis of their functions, and the identification of interactions among them. Detailed characterization of these interactions then becomes central to gain a true mechanistic understanding. Ultimate goals of these studies are often to reconstitute the relevant complexes with purified components, to determine their three-dimensional structures, and to reveal how rearrangements between complexes underlie the biology of the system. Accomplishing these goals requires the application of very diverse techniques and therefore involves the participation of scientists with different expertise. The resulting interdisciplinary interactions can be extremely stimulating, but integrating the information obtained with different approaches is hampered by the distinct views and languages characteristic of different disciplines.

This review has the double purpose of offering our perspective on the study of molecular mechanisms as biophysicists and of providing an overview on how these mechanisms are elucidated through the analysis of protein interactions by nuclear magnetic resonance (NMR) spectroscopy in combination with other biophysical techniques. We hope that this review will be useful to NMR spectroscopists and biophysicists interested in the study of protein interactions, and will also be helpful for researchers from other disciplines to understand biophysical studies of molecular mechanisms. This is a very broad area and attempting to give a comprehensive account would be impractical. Instead, we focus largely on what we have learned from our experiences, presenting case studies on neurotransmitter release that illustrate a variety of principles. We start with a brief description of the neurotransmitter release machinery. Later we discuss some general considerations on the analysis of protein interactions and some concepts on basic NMR experiments that are particularly powerful to study protein interactions, before going into the case studies. From the outset, we would like to emphasize that all techniques have advantages and limitations, and hence it is critical to combine approaches that provide complementary information.

The neurotransmitter release machinery

Neurotransmitter release is a key event in interneuronal communication. Release involves a series of steps that include the docking of synaptic vesicles to presynaptic active zones, priming to a release-ready state and Ca^{2+}-triggered fusion of the vesicle and plasma membranes (Sudhof, 2004). Central components of the release machinery are N-ethylmaleimide-sensitive factor (NSF), soluble NSF attachments proteins (SNAPs), the soluble SNAP receptor (SNARE) proteins syntaxin-1, synaptobrevin and synaptosomal protein of 25 kDa (SNAP-25; no relation to SNAPs), and the Sec1/Munc18 (SM) protein Munc18-1 (Brunger, 2005; Jahn and Scheller, 2006; Rizo and Rosenmund, 2008; Sudhof and Rothman, 2009). These proteins or their homologs mediate membrane fusion at most intracellular membrane compartments, underlying a universal mechanism of fusion. The three SNAREs form a tight 'SNARE complex' that bridges the vesicle and plasma membranes (Supplementary Figure S1; Sollner et al., 1993a; Hanson et al., 1997), which is key for fusion, while Munc18-1 is also crucial for release (Verhage et al., 2000), cooperating with the SNAREs in fusion. NSF and SNAPs disassemble the SNARE complex to recycle the SNAREs (Sollner et al., 1993a; Banerjee et al., 1996; Mayer et al., 1996). Synaptic vesicle fusion is also governed by Rab3s, small GTPases from the Rab family that normally mediate vesicle docking and targeting specificity (Cai et al., 2007).

The regulation of release also depends on specialized proteins such as the large active zone proteins Munc13-1 and RIM, which are critical for synaptic vesicle priming (Augustin et al., 1999; Richmond et al., 1999; Koushika et al., 2001; Schoch et al., 2002), the synaptic vesicle synaptotagmin-1, which acts as a Ca^{2+} sensor (Fernandez-Chacon et al., 2001), and complexins, which bind tightly to the SNARE complex (McMahon et al., 1995) and play important roles in priming and Ca^{2+} triggering of release (Reim et al., 2001; Xue et al., 2010; Yang et al., 2010). A common feature of synaptotagmin-1, Munc13-1, RIM, and other proteins involved in the release is the presence of C_2 domains in their sequences (referred to as C_2A, C_2B, etc.). These domains normally function as Ca^{2+} and phospholipid-binding modules, but can also act as protein–protein interaction domains and sometimes do not bind Ca^{2+} (Rizo and Sudhof, 1998).

General considerations on the study of protein interactions

The identification of protein interactions forms an intrinsic part of the initial characterization of a biological system. Several methods based on affinity chromatography on a solid support are widely employed for this purpose, taking advantage of antibody/antigen binding in immunoprecipitations (IPs) or protein/small molecule interactions in pulldown assays (e.g. with immobilized GST-fusion proteins). These methods led to fundamental discoveries on the release machinery. For instance, the cloning of synaptotagmin-1 (Perin et al., 1990) allowed the use of affinity chromatography to purify syntaxin-1 (Bennett et al., 1992). In turn, this protein was used to isolate Munc18-1 (Hata et al., 1993) and complexins (McMahon et al., 1995). This approach also identified a complex of NSF and SNAPs with syntaxin-1, synaptobrevin and SNAP-25, which lead to their designation as SNAREs (Sollner et al., 1993b) and eventually to the finding

that they form the SNARE complex (Sollner et al., 1993a). The yeast-two-hybrid (Y2H) method is also used extensively to find binding partners of a protein. This approach becomes a particularly useful alternative to affinity chromatography-based techniques when the known protein is insoluble or difficult to handle biochemically. For instance, Y2H assays were key to finding proteins that bind to RIMs, which are central components of the highly insoluble cytomatrix of presynaptic active zones (Betz et al., 2001; Schoch et al., 2002; Kaeser et al., 2011).

While pulldowns, IPs and Y2H assays have been used successfully in innumerable cases, we often find that bona fide interactions were not detected by these methods or interactions observed by these methods cannot be reproduced with purified, well-characterized proteins (e.g. Fernandez et al., 2001; Ubach et al., 2001; Basu et al., 2005; Dai et al., 2005; Dulubova et al., 2007; Guan et al., 2007, 2008). These inconsistencies can arise for a variety of reasons. For example, the fusion of a protein to another polypeptide (for pulldowns or Y2H assays) or binding of a protein to an antibody can create steric hindrance and prevent binding to a relevant target. Conversely, weak, non-specific interactions of the protein with an irrelevant factor might be enhanced by cooperativity with weak interactions of the irrelevant factor with the antibody, the fused polypeptide or the resin itself. This issue is of particular concern when binding is performed with a large excess of immobilized protein and detected by immunoblotting with antibodies to a putative target, since these methods can detect even a very small amount of binding and hence are more likely to yield artifacts unless the interaction is proved to be saturable and stoichiometric. Misleading results are also likely in experiments performed with insufficiently characterized protein fragments. Thus, fragments that aggregate or misfold because they do not correspond to a complete folding module are often found to make non-specific interactions with many targets. Moreover, fusion proteins that are isolated by affinity chromatography without further purification might contain non-protein contaminants that are not detectable by the typical methods used to determine protein purity. Such contaminants can mask binding to physiological targets and/or mediate indirect binding to irrelevant factors. These problems can be particularly severe for proteins that are highly positively charged and thus bind tightly to DNA or RNA [e.g. the synaptotagmin-1 C_2B domain (Fernandez et al., 2001; Ubach et al., 2001)].

Common problems in studies of protein–protein interactions can also arise from the existence of intramolecular interactions, from the promiscuity of some proteins, or from the weak nature of many physiological interactions. Intramolecular interactions between domains of one protein can hinder intermolecular binding to a target, leading to inconsistent results when different fragments are used [e.g. for syntaxin-1 (Calakos et al., 1994; Dulubova et al., 1999; Hazzard et al., 1999)]. Protein promiscuity can be a serious problem in some cases. For instance, syntaxin-1 has been reported to bind to more than 50 other proteins (Jahn and Scheller, 2006; Rizo and Rosenmund, 2008), many of which are unlikely to be relevant targets [e.g. syntaxin-1 co-immunoprecipitates with potassium channels that do not reside in the same subcellular compartment (Fletcher et al., 2003)]. Conversely, weak but relevant physiological interactions

may not be detected in co-IPs or pulldown assays if the off-rates are fast and bound targets are lost during the resin washing steps. This issue poses an important problem because many regulatory interactions are relatively weak. Interesting alternatives to the pulldown assays to overcome some of their problems and facilitate the detection of weak interactions are the 'holdup' and the 'catchup' assays (Charbonnier et al., 2006).

After their initial identification, protein interactions should be verified using purified proteins that are well characterized (e.g. by chromatography, UV spectroscopy, and some biophysical techniques). Native gel electrophoresis and gel filtration offer simple tools to test whether two proteins bind *in vitro*. These methods have the advantage that they do not require tags, but normally they only detect relatively tight interactions ($K_d \leq 1\ \mu M$). A wide variety of biophysical techniques are available to test protein interactions, to determine their stoichiometry and affinity, and/or to characterize their nature at different levels of detail. Some of the most used techniques are isothermal titration calorimetry (ITC), analytical ultracentrifugation, fluorescence anisotropy, fluorescence resonance energy transfer (FRET), circular dichroism (CD), dynamic light scattering (DLS), multi-angle laser light scattering, small angle X-ray scattering, electron paramagnetic resonance (EPR), surface plasmon resonance, electron microscopy (EM), NMR spectroscopy and X-ray crystallography. Each of these techniques provides different types of information and suffers from different drawbacks; hence, it is always advisable to use them in combination. For instance, ITC is the method of choice for thermodynamic analysis of protein interactions but requires relatively high protein concentrations, typically micromolar and measurable heats of binding. On the other hand, FRET and fluorescence anisotropy are highly sensitive and provide structural and mobility information, respectively, but usually require the attachment of fluorescence probes that could hinder or enhance an interaction.

X-ray crystallography, NMR spectroscopy, EM and EPR are the main tools used to characterize protein interactions at or near atomic resolution, which provides a fundamental framework to elucidate molecular mechanisms. However, even these powerful techniques can lead to misleading results (see examples below). Importantly, all these techniques are normally applied *in vitro* and it is crucial to verify that the protein interaction under study is physiologically relevant. In our opinion, the most definitive approach for this purpose involves the design of point mutations that disrupt or enhance the interaction and the establishment of quantitative correlations between the effects of these mutations on binding *in vitro* and their functional effects *in vivo* [e.g. synaptotagmin-1 (Fernandez-Chacon et al., 2001; Rhee et al., 2005), see below]. As a final consideration, we note that bona fide interactions of a protein from one species and cellular compartment cannot be assumed to be conserved in homologs of the protein in other species or compartments, as underscored by the properties of syntaxins (see below) and by the distinct Ca^{2+}-binding properties of synaptotagmin-4 from rat and *Drosophila* (Dai et al., 2004).

Interpretation of two-dimensional heteronuclear NMR spectra

Discussing methods for structure determination is beyond the scope of this review, but in this section we summarize a few concepts on two-dimensional (2D) heteronuclear NMR experiments that can quickly yield a wealth of information on protein interactions. These concepts will illustrate the power of these experiments and will help non-experts understand some of the NMR data described in the case examples.

^1H-^{15}N heteronuclear single quantum coherence (HSQC) spectra of ^{15}N-labeled proteins, which are widely used, correlate directly bonded pairs of ^1H and ^{15}N nuclei and hence yield one cross-peak for the backbone amide group of each non-proline residue of a protein, as illustrated by the ^1H-^{15}N HSQC spectrum of the C_2B domain from the Rab3 effector rabphilin (Ubach et al., 1999; Supplementary Figure S2A). The excellent dispersion of this spectrum is common for well-folded proteins because their amide groups have unique chemical environments. ^1H-^{15}N HSQC spectra are thus like protein fingerprints and changes in these fingerprints report on binding interactions or structural changes. Binding of a small ligand typically induces selective shifts in the cross-peaks from residues near the binding site, thus revealing the site. This is illustrated in Supplementary Figure S2B for Ca^{2+} binding to the rabphilin C_2B domain, which causes shifts selectively in the cross-peaks from residues near its Ca^{2+}-binding region (Ubach et al., 1999). Note, however, that chemical shift changes resulting from conformational changes that propagate from the binding site cannot be deconvoluted from those reflecting direct protein–protein contacts. Therefore, chemical shift mapping experiments must be interpreted with caution.

Titrations can yield additional information from ^1H-^{15}N HSQC spectra. If the exchange rate is fast compared with the changes in chemical shift induced by binding (which can range from 0 to 1000 Hz, or even higher), the cross-peaks gradually move from their free-state positions to the bound-state positions during the titration. This is illustrated by the cross-peak highlighted in red in Supplementary Figure S2C, which shows superimposed expansions of ^1H-^{15}N HSQC spectra of the synaptotagmin-1 C_2A domain acquired with increasing Ca^{2+} concentrations. Thus, the red cross-peak moves gradually from the Ca^{2+}-free to the Ca^{2+}-bound position. The titration revealed three components with movement in different directions, reflecting consecutive binding of Ca^{2+} at three distinct but nearby sites with distinct affinities (Ubach et al., 1998). The patterns of cross-peak movements provided key clues to elucidate the three Ca^{2+}-binding sites, which were then verified by mutagenesis. For instance, the third component of the titration was lost after mutating a ligand (S235) that coordinates only the site with lowest affinity (Supplementary Figure S2D).

If the exchange rate is in an intermediate regime, i.e. if binding and dissociation kinetics are comparable to the changes in chemical shift induced by the interaction, binding leads to cross-peak broadening (referred to as chemical exchange broadening). This behavior can also be used to map the binding site. If the exchange regime is slow, the ^1H-^{15}N HSQC cross-peaks from the free state disappear gradually and those from the bound state appear gradually, as illustrated in Supplementary Figure S2E and F, by a Ca^{2+} titration of the C_2A domain from the active-zone protein piccolo (Gerber et al., 2001). Slow exchange regimes are normally associated with high-affinity binding (e.g. $K_d < 1\ \mu M$), but can also occur for low-affinities if ligand binding requires a conformational

change. In the case of the piccolo C_2A domain, the Ca^{2+} affinity is in the low mM range (Supplementary Figure S2F), but a large conformational change is required for Ca^{2+} binding to occur (Garcia et al., 2004). Note that substantial conformational changes upon ligand binding normally lead to widespread changes in the ^1H-^{15}N HSQC spectra (e.g. Supplementary Figure S2E), which prevents definition of the ligand-binding site by this method.

^1H-^{15}N HSQC spectra can also be used to map the region of a ^{15}N-labeled protein that binds to an unlabeled protein. In these studies, in addition to inducing chemical shift changes and/or chemical exchange broadening, binding should cause overall broadening of NMR signals due to the increased size of the complex with respect to the isolated ^{15}N-labeled protein. Such broadening limits the size of the protein complexes that can be studied, but transverse relaxation optimized spectroscopy (TROSY) dramatically alleviated this problem, allowing the study of complexes of 100 kDa and beyond (Riek et al., 2002). The overall broadening caused by binding of an unlabeled protein should in principle extend to most cross-peaks from the ^{15}N-labeled protein, but cross-peaks from flexible regions may remain largely unaffected if they are not involved in binding because internal motions lead to very sharp resonances for flexible regions regardless of the molecular size. A dramatic example of this notion is provided by the ^1H-^{15}N HSQC spectrum of the synaptic vesicle SNARE synaptobrevin (116 residues) reconstituted into 100 nm lipid vesicles (Brewer et al., 2011). Even though the effective molecular weight of the vesicles is in the 100-MDa range, the ^1H-^{15}N HSQC cross-peaks of residues $1-74$ are still observable with high sensitivity even at $9~\mu M$ protein concentration because these residues remain flexible (Supplementary Figure S2G, red contours). This feature can be used to identify flexible tails in proteins and remove them to facilitate crystallization (e.g. Guan et al., 2007).

The concepts discussed above also apply to other types of 2D heteronuclear NMR experiments. Increasingly used are ^1H-^{13}C methyl HMQC (methyl TROSY) spectra of highly deuterated proteins that are selectively ^1H,^{13}C-labeled at Ile, Val, Leu and/or Met methyl groups (below referred to as ^2H,$^{13}CH_3$-IVLM labeling, where IVLM may change depending on the residues that are $^{13}CH_3$ labeled; Rosen et al., 1996; Gardner and Kay, 1998; Ruschak and Kay, 2010). These spectra have very high sensitivity even for large protein complexes, as shown by studies of $0.2-1$ MDa complexes (Kreishman-Deitrick et al., 2003; Sprangers and Kay, 2007; Gelis et al., 2007; see also below). Heteronuclear 2D NMR experiments are also useful to detect intramolecular interactions within proteins, as shown for syntaxin-1 below (Dulubova et al., 1999) and by other examples (e.g. Kim et al., 2000; Harper et al., 2003). In addition, these experiments can be acquired in one-dimensional (1D) mode (referred to as 1D ^{15}N- or ^{13}C-edited ^1H-NMR spectra) with very high sensitivity even at low micromolar protein concentrations because the ^1H signals are not dispersed into a second dimension (Arac et al., 2003; Dulubova et al., 2005; Ma et al., 2011). Monitoring the decrease in signal intensities in these spectra upon addition of an unlabeled protein provides a facile tool to monitor binding and determine the affinity of the interaction.

Coupling between SNARE and Munc18-1 function

The SM protein Munc18-1 and the SNARE proteins syntaxin-1, SNAP-25 and synaptobrevin form part of the core machinery that controls neurotransmitter release (Supplementary Figure S1; Rizo and Rosenmund, 2008; Sudhof and Rothman, 2009). The SNAREs contain ca. 65-residue sequences called SNARE motifs. Synaptobrevin and syntaxin-1 each contain one SNARE motif preceding a C-terminal transmembrane (TM) region that is anchored to the vesicle or plasma membrane, respectively; SNAP-25 contains two SNARE motifs. CD and NMR data revealed that the isolated SNARE motifs are largely unstructured (Fasshauer et al., 1997; Dulubova et al., 1999; Hazzard et al., 1999). EM and FRET studies showed that the SNARE motifs of synaptobrevin and syntaxin-1 bind in a parallel fashion, leading to the notion that SNARE complex assembly brings the vesicle and plasma membranes together and is key for membrane fusion (Hanson et al., 1997; Lin and Scheller, 1997). EPR and X-ray crystallography showed that the SNARE complex consists of a parallel four-helix bundle formed by the four SNARE motifs of synaptobrevin, syntaxin-1 and SNAP-25 (Poirier et al., 1998; Sutton et al., 1998; Figure 1A).

Syntaxin-1 contains an N-terminal region that was shown by NMR spectroscopy to include a three-helix bundle (the H_{abc} domain; Fernandez et al., 1998; Figure 1A). Comparison of the ^1H-^{15}N HSQC spectra of syntaxin-1 fragments spanning the isolated H_{abc} domain or the H_{abc} domain plus the SNARE motif revealed shifts in multiple cross-peaks of the H_{abc} domain (Figure 1B), showing that syntaxin-1 forms a 'closed conformation' where the H_{abc} domain binds intramolecularly to the SNARE motif (Dulubova et al., 1999). This closed conformation is incompatible with the SNARE complex, explaining why syntaxin-1 binding to synaptobrevin was observed in the absence but not in the presence of the H_{abc} domain (Calakos et al., 1994; Hazzard et al., 1999).

Functional and reconstitution studies supported the notion that the SNAREs are crucial for membrane fusion, but a fundamental question is how their function is coupled to Munc18-1 (Rizo and Rosenmund, 2008; Sudhof and Rothman, 2009). Munc18-1 binds very tightly to isolated syntaxin-1 (Hata et al., 1993) [$K_d = 1.4$ nM by ITC (Burkhardt et al., 2008)]. ^1H-^{15}N HSQC spectra revealed that a mutation in syntaxin-1 that impairs Munc18-1 binding (called 'LE mutation') disrupts the closed conformation, showing that the syntaxin-1 closed conformation binds to Munc18-1 (Dulubova et al., 1999). The crystal structure of the syntaxin-1/Munc18-1 complex revealed that Munc18-1 contains three domains and forms an arch shape with a cavity that binds to closed syntaxin-1 (Misura et al., 2000; Figure 1C). Correspondingly, Munc18-1 binding to syntaxin-1 hinders SNARE complex formation (Dulubova et al., 1999; Burkhardt et al., 2008; Ma et al., 2011), and knockin mice bearing the LE mutation in syntaxin-1 exhibit an increase in the synaptic vesicle release probability, supporting the physiological relevance of the closed conformation and its autoinhibitory role (Gerber et al., 2008).

While important, these results did not explain why Munc18-1 is essential for neurotransmitter release (Verhage et al., 2000). Furthermore, the SM protein Sec1p (the yeast homolog of
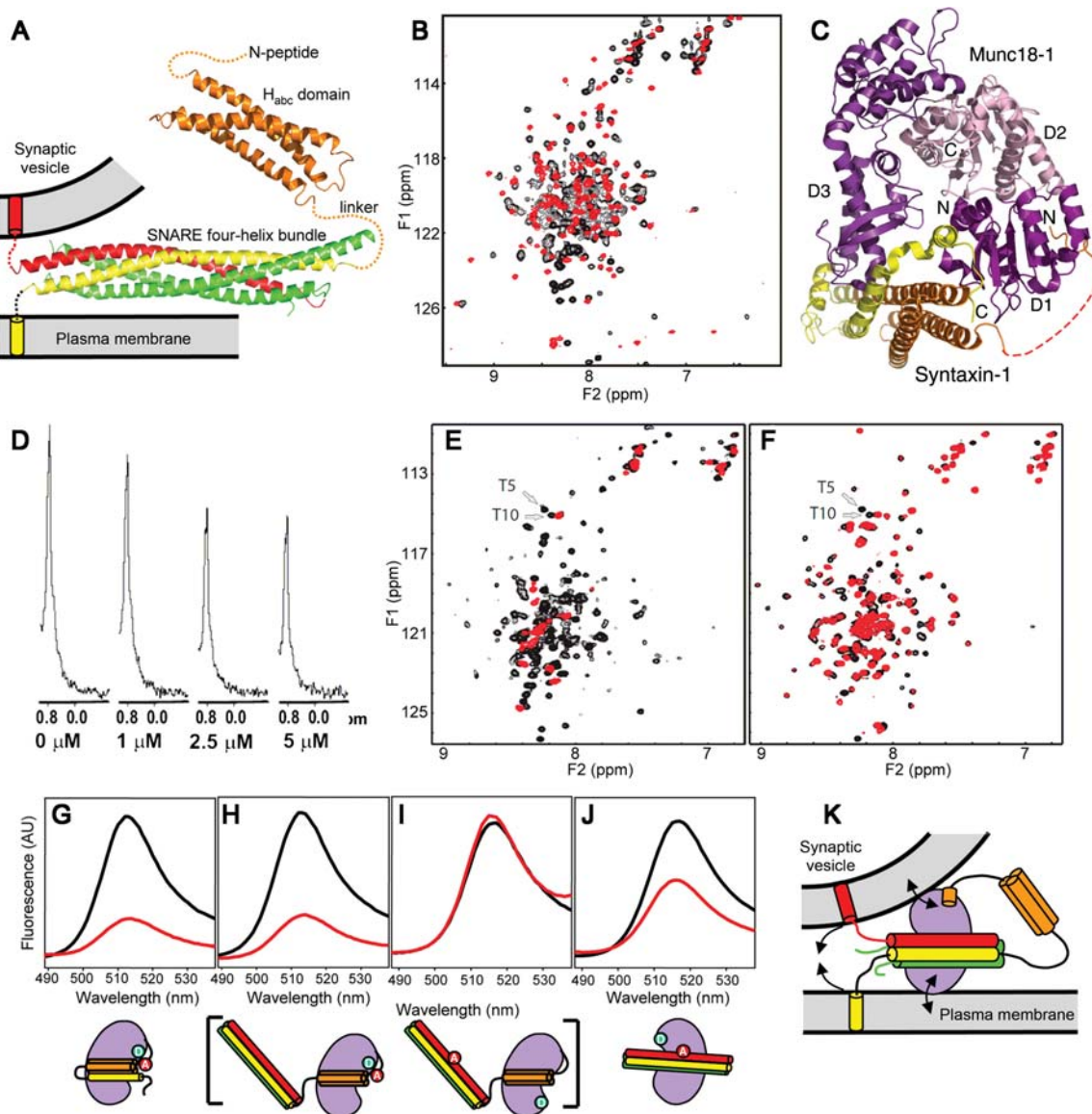
Figure 1 Munc18-1/SNARE coupling. (**A**) Ribbon diagrams of the syntaxin-1 H_{abc} domain (orange; Fernandez et al., 1998) and the SNARE complex four-helix bundle (syntaxin-1 yellow, SNAP-25 green, SNAP-25 red; Sutton et al., 1998); TM regions are represented by cylinders and other sequences by dashed curves. (**B**) ^1H-^{15}N HSQC spectra of the syntaxin-1 H_{abc} domain (residues 27−146; red) and of a longer fragment including the SNARE motif (residues 26−253; black; Dulubova et al., 1999). (**C**) Ribbon diagram of the Munc18−1/closed syntaxin-1 complex (Burkhardt et al., 2008). The three domains of Munc18-1 (D1-D3) are in different shades of purple. The syntaxin-1 linker and SNARE motif are in yellow; the N-peptide (labeled N) and H_{abc} domain are in orange, and the sequence between them (not observable) is represented by a dashed curve. (**D**) 1D ^{13}C-edited ^1H-NMR spectra of ^{13}C-labeled Munc18-1 in the absence and presence of different concentrations of unlabeled SNARE complex (below the spectra). Modified from Dulubova et al. (2007), copyright (2007) National Academy of Sciences, USA. (**E**) ^1H-^{15}N HSQC spectra of the syntaxin-1 cytoplasmic region in the absence (black) and presence (red) of Munc18-1. Spectra were plotted at high contour levels to emphasize the strong cross-peaks of flexible regions of syntaxin-1 and illustrate how the cross-peaks of residues T5 and T10 from the flexible N-peptide are broadened beyond detection upon binding to Munc18-1. (**F**) ^1H-^{15}N HSQC spectra of the syntaxin-1 N-terminal region (residues 2−180) in the absence (black) and presence (red) of the Munc18-1 N-terminal domain. Panels **E** and **F** modified with permission from Khvotchev et al. (2007). (**G**−**J**) Emission fluorescence spectra of Munc18-1 labeled with BODIPY before (black) or after (red) binding to closed syntaxin-1 (**G**), the SNARE complex (**H** and **I**), or the SNARE four-helix bundle (**J**) containing acceptor probes. Models below the spectra illustrate the binding modes of the complexes and the approximate locations of the fluorescence probes (color coding as in panels **A** and **C**). Panels **G**−**J** adapted with permission from Xu et al. (2010), copyright (2010) American Chemical Society. (**K**) The model of how Munc18-1 and the SNAREs could cooperate in membrane fusion. The key aspect of this model is that Munc18-1 (purple) bound to the assembling SNARE four-helix bundle prevents the approximation of the synaptic vesicle and plasma membranes (gray) at the same time that the SNAREs pulls them together; the resulting combination of forces (illustrated by the arrows) bends the two membranes to initiate membrane fusion (Rizo et al., 2006; Dulubova et al., 2007; Xu et al., 2010).

Munc18-1) was found to bind to the SNARE complex instead of its cogante syntaxin (Carr et al., 1999), and NMR and other biophysical data showed that only a subset of syntaxins adopt a closed conformation (Nicholson et al., 1998; Fiebig et al., 1999; Dulubova et al., 2001, 2002; Yamaguchi et al., 2002; Furgason et al., 2009). Furthermore, syntaxins from several membrane compartments were found to bind to their cognate SM proteins through a sequence at the very N-terminus (called N-peptide; Bracher and Weissenhorn, 2002; Dulubova et al., 2002; Yamaguchi et al., 2002). This confusing picture was partially reconciled by the discovery that, contrary to previous conclusions from GST pulldowns (Yang et al., 2000), Munc18-1 binds to the SNARE complex, as demonstrated by several methods including the decreased intensity of 1D ^{13}C-edited ^{1}H-NMR spectra of ^{13}C-labeled Munc18-1 upon addition of the SNARE complex (Figure 1D; Dulubova et al., 2007; Shen et al., 2007). Titrations using these spectra yielded a K_d of ca. 300 nM (Dulubova et al., 2007; Deak et al., 2009).

These results and data from other systems (Carpp et al., 2006; Latham et al., 2006; Stroupe et al., 2006) suggest that all SM proteins bind to SNARE complexes and that this interaction underlies the crucial role of SM proteins in membrane fusion, as predicted by a model of how SM proteins cooperate with the SNAREs in fusion (Rizo et al., 2006). However, the nature and mechanism of action of Mun18-1/SNARE complex assemblies are still unclear. The syntaxin-1 N-peptide is key for Munc18-1 binding to the SNARE complex with submicromolar affinity (Dulubova et al., 2007) and was not observed initially in the crystal structure of the binary syntaxin-1/Munc18-1 complex (Misura et al., 2000). However, ^{1}H-^{15}N HSQC spectra showed that the syntaxin-1 N-peptide does participate in the binary complex (Khvotchev et al., 2007; Figure 1E), which was confirmed by reanalysis of the X-ray data (Burkhardt et al., 2008; Figure 1C). Interestingly, the perturbations in ^{1}H-^{15}N HSQC spectra of the syntaxin-1 N-terminal region caused by the Munc18-1 N-terminal domain (Figure 1F) suggested that these two fragments bind in a similar mode as in the Munc18-1/syntaxin-1 complex (Khvotchev et al., 2007). These results and ITC data (Burkhardt et al., 2008) suggest that the interactions of the syntaxin-1 N-peptide and H_{abc} domain with Munc18-1 present in the binary complex underlie the binding of the SNARE complex to Munc18-1 (see models in Figure 1G−I). The crucial functional significance of these interactions has been supported by multiple evidence (Khvotchev et al., 2007; McEwen and Kaplan, 2008; Deak et al., 2009; Rathore et al., 2010).

NMR and biochemical data indicated that Munc18-1 also binds to the SNARE four-helix bundle (Dulubova et al., 2007; Shen et al., 2007), but it was unclear whether this interaction is compatible with binding to the syntaxin-1 N-terminal region. Studies with donor and acceptor fluorescence probes on Munc18-1 and syntaxin-1, placed at locations that are close in the syntaxin-1/Mun18-1 complex, yielded strong FRET when Munc18-1 bound to either syntaxin-1 or to the SNARE complex (Figure 1G and H; Xu et al., 2010). Placing the acceptor probe on synaptobrevin to monitor binding of Munc18-1 to the SNARE four-helix bundle did not yield FRET if the SNARE complex included the syntaxin-1 N-terminal region (Figure 1I), but FRET was observed when the

isolated four-helix bundle was used (Figure 1J). These and other results (Shen et al., 2010) suggest that the syntaxin-1 N-terminal region and the SNARE four-helix bundle compete for binding to Munc18-1, leading to a model whereby Munc18-1 transits through at least three different types of interactions with the SNAREs. In this model, Munc18-1 first binds to closed syntaxin-1, which inhibits release and provides a key point of regulation (Figure 1G); when syntaxin-1 opens, Munc18-1 remains bound to the syntaxin-1 N-terminal region (Figure 1H and I), and later Munc18-1 translocates to the SNARE four helix bundle (Figure 1J; Xu et al., 2010). Such translocation could be facilitated by interactions with the membranes, as suggested by some biochemical data (Shen et al., 2007), and could allow Munc18-1 to cooperate with the SNARE complex in applying force to bend the membranes and initiate fusion (Figure 1K; Rizo et al., 2006). This model is still tentative but, regardless of the validity of the model, studies of Munc18-1-SNARE interactions provide a vivid illustration of the complexities entailed in elucidating molecular mechanisms involving interactions between different regions of the same proteins, particularly when some of these interactions are weak, depend on other factors (e.g. membranes), and change during the different steps of the biological process. At the same time, this research underlines the power of biophysical methods to unravel complex mechanisms and guide further biological studies.

Opening syntaxin-1 with Munc13s

Mammalian Munc13s and their invertebrate homolog Unc13 play a key role in priming synaptic vesicles to a release-ready state (Augustin et al., 1999; Richmond et al., 1999). A role for these proteins in opening syntaxin-1 was suggested by the finding that the open syntaxin-1 LE mutant partially rescues the priming defects of Unc13 null mutants (Richmond et al., 2001), and a large C-terminal region called the MUN domain was found to form a folded module that is responsible for the priming function of Munc13-1 (Basu et al., 2005).

Liposome co-floatation and single molecule fluorescence studies showed that the MUN domain binds to membrane-anchored SNARE complexes or syntaxin-1-SNAP-25 heterodimers, which involves the cooperation of weak interactions of the MUN domain with the SNAREs and the membranes (Guan et al., 2008; Weninger et al., 2008). Heteronuclear 1D and 2D NMR experiments then showed that the MUN domain binds weakly to the soluble SNARE complex and very weakly to Munc18-1, and that both interactions also cooperate with each other (Ma et al., 2011). Figure 2A illustrates how ^{1}H-^{13}C HMQC spectra of 12 μM ^{2}H,^{13}CH$_3$-IVL-labeled MUN domain (73 kDa) exhibit high sensitivity, and how binding of Munc18-1 (68 kDa) and the SNARE complex (55 kDa) induces strong broadening but most cross-peaks of the resulting 200 kDa complex are still observable. ^{1}H-^{15}N HSQC experiments showed that the MUN domain also binds weakly to the syntaxin-1 SNARE motif, mapping the binding site to residues 200−226 (Ma et al., 2011; Figure 2B). These results suggested a model whereby binding of the MUN domain to the syntaxin-1 SNARE motif, and perhaps to Munc18-1, could 'extract' the SNARE motif from the closed syntaxin-1-Munc18-1 complex and provide a template to assemble the SNARE complex (Figure 2C).
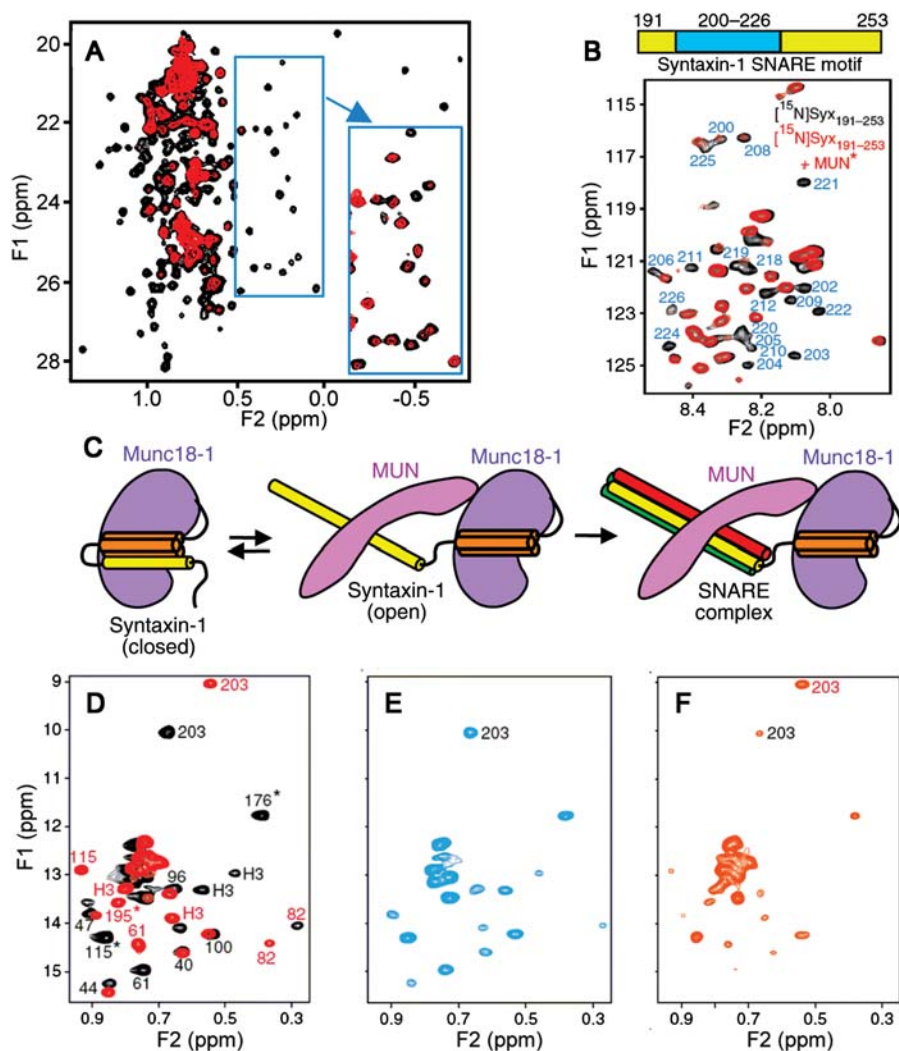
Figure 2 MUN-domain function. (**A**) ^{1}H-^{13}C HMQC spectra of ^{1}H,^{13}C-IVL-^{2}H-labeled Munc13-1 MUN domain in the absence (black) and presence (red) of Munc18-1 and the SNARE complex. The expansion in the inset was plotted at lower contour levels to allow the observation of the weaker cross-peaks. (**B**) ^{1}H-^{15}N HSQC spectra of the syntaxin-1 SNARE motif in the absence (black) and presence (red) of the Munc13-1 MUN domain. The assignments of cross-peaks that disappear upon MUN-domain binding are indicated with the residue number; they correspond to residues 200–226 (diagram above). (**C**) Model of how the MUN domain (pink) helps to open syntaxin-1 by binding to its SNARE motif (yellow) and providing a template to assemble the SNARE complex. (**D**) ^{1}H-^{13}C HMQC spectra of ^{1}H,^{13}C-I-^{2}H-labeled syntaxin-1 bound to Munc18-1 (black) or forming the SNARE complex (red). Cross-peak assignments are indicated (H3 = SNARE motif). (**E** and **F**) Analogous spectra acquired on the syntaxin-1/Munc18-1 complex after the addition of the synaptobrevin and SNAP-25 SNARE motifs in the absence (**E**) and presence (**F**) of MUN domain. All panels reproduced from Ma et al. (2011).

This model was validated with ^{1}H-^{13}C HMQC spectra of 15 μM ^{13}CH$_3$-I-labeled syntaxin-1, which allowed to distinguish between its complex with Munc18-1 and the SNARE complex (Figure 2D). ^{1}H-^{13}C HMQC spectra acquired as a function of time showed that, starting with ^{13}CH$_3$-I-labeled syntaxin-1 bound to Munc18-1, the formation of the SNARE complex with synaptobrevin and SNAP-25 was very slow, but the addition of the MUN domain accelerated SNARE complex assembly 100-fold (Ma et al., 2011; Figure 2E and F). Analogous results were obtained using FRET assays, which in addition showed that the accelerating activity of the MUN domain was abolished by a point mutation that disrupts the MUN domain/syntaxin-1 SNARE motif interaction. These results showed that the MUN domain mediates the transition from the closed syntaxin-1/Munc18-1 complex to the SNARE complex, emphasized the importance that weak interactions can have in biological processes, and illustrated the power of NMR spectroscopy to monitor complicated rearrangements in multiprotein complexes. It is worth noting that additional events may occur after syntaxin-1 opens, including the translocation of Munc18-1 to the SNARE four-helix bundle (see above), and that computational analyses and the crystal structure of part of the MUN domain showed that this domain is related to tethering factors involved in traffic at diverse membrane compartments (Pei et al., 2009; Li et al., 2011). This finding suggests that the MUN domain may have an additional function that is shared with tethering complexes,

perhaps cooperating with Munc18-1 and the SNAREs in membrane fusion.

Complexin–SNARE interactions

Complexins are small (ca. 16 kDa) soluble proteins that bind tightly to the SNARE complex (McMahon et al., 1995), and play both active and inhibitory roles in neurotransmitter release (Reim et al., 2001; Tang et al., 2006; Huntwork and Littleton, 2007; Xue et al., 2007; Maximov et al., 2009). ^{1}H-^{15}N HSQC spectra showed that complexin-1 is largely unstructured in solution but its central sequences populate α-helical conformation and, together with biochemical assays, revealed that these central sequences are key for SNARE complex binding (Pabst et al., 2000). ^{1}H-^{15}N TROSY-HSQC spectra of a ^{2}H,^{15}N-labeled complexin-1 central fragment showed that a subset of cross-peaks become well dispersed upon binding to the SNARE complex (Figure 3A), and ^{1}H-^{15}N TROSY-HSQC spectra of SNARE complexes where syntaxin-1 or synaptobrevin was ^{2}H,^{15}N-labeled exhibited shifts of selected cross-peaks upon complexin-1 binding (Figure 3B and C), whereas much smaller perturbations occurred in analogous spectra with the SNAP-25 SNARE motifs ^{2}H,^{15}N-labeled (Chen et al., 2002).

These results mapped the approximate regions involved in complexin-1/SNARE interactions, and the solubility optimization performed to improve the NMR data facilitated co-crystallization of the complexin-1 fragment with the SNARE complex. The crystal structure of the complex showed that a central helix of complexin-1 binds in an antiparallel orientation to the synaptobrevin and syntaxin-1 SNARE motifs, and that a sequence preceding the central complexin-1 helix is also helical but does not contact the SNAREs (called accessory helix; Figure 3D; Chen et al., 2002). This binding mode was fully compatible with the NMR data, which thus provided an important validation for the crystal structure as the high percentage of organic solvent in the crystals might have distorted the complex. Deuterium exchange experiments monitored by ^{1}H-^{15}N TROSY-HSQC spectra showed that complexin-1 binding stabilizes the SNARE complex, which likely underlies in part the active role of complexins in neurotransmitter release (Chen et al., 2002). These results provided a clear illustration of the power of combining NMR
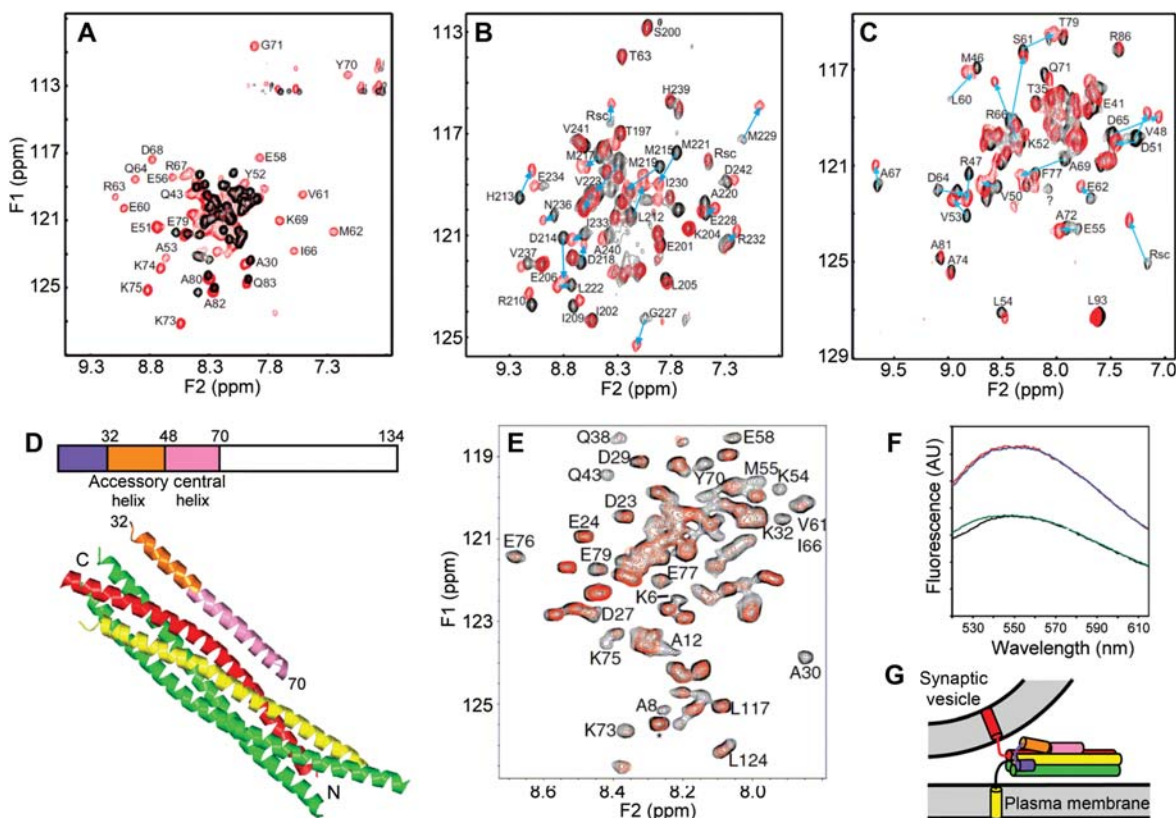

Figure 3 Complexin/SNARE interactions. (**A**) ^{1}H-^{15}N TROSY-HSQC spectra of a ^{2}H,^{15}N-labeled complexin-1 (residues 26–83) in the absence (black) and presence (red) of unlabeled SNARE four-helix bundle. (**B** and **C**) ^{1}H-^{15}N TROSY-HSQC spectra of the SNARE four-helix bundle ^{2}H,^{15}N-labeled at the syntaxin-1 (**B**) or synaptobrevin (**C**) SNARE motif in the absence (black) and presence (red) of unlabeled complexin-1 (residues 26–83). Panels **A**–**C** reprinted from Chen et al. (2002), Copyright (2002), with permission from Elsevier. (**D**) Domain diagram of complexin-1 and structure of the complexin-1 (26–83)/SNARE complex (Chen et al., 2002). (**E**) Expansions of ^{1}H-^{15}N HSQC spectra of 2 μM ^{15}N-labeled complexin-1 in the absence (black) and presence (red) of liposomes containing reconstituted SNARE complex (3 μM). (**F**) Fluorescence spectra of complexin-1 labeled with 7-nitrobenz-2-oxa-1,3-diazole at residue 12 in the absence (black) or presence of liposomes (green), soluble SNARE complex (red) or SNARE complex-containing liposomes (blue). Increased fluorescence indicates the binding of the complexin-1 N-terminus to the SNARE complex. (**G**) Working model of how complexin binds to the SNARE complex. The complexin-1 N-terminus (blue) binds to the C-terminus of the SNARE complex, but the location of the binding site is unclear. Panels **E**–**G** modified from Xue et al. (2010).

spectroscopy and X-ray crystallography to study molecular mechanisms.

Mutagenesis and electrophysiological studies demonstrated that binding to the SNARE complex through the central helix is crucial for the active function of complexin-1 in release and in addition showed that the N-terminus is also key for this function, while the accessory helix has an inhibitory role (Xue et al., 2007; Maximov et al., 2009). Based on the location of the accessory helix in the crystal structure (Figure 3D), it was proposed that part of this helix might inhibit release by interfering with assembly of the C-terminus of the SNARE complex (Xue et al., 2007). This model was supported by some data (Giraudo et al., 2009; Lu et al., 2010), but results obtained with a complexin triple mutant suggested an alternative model of interference with SNARE complex C-terminal assembly (Kummel et al., 2011), and the mechanism of inhibition is still unclear. On the other hand, ^{1}H-^{15}N HSQC spectra of 2 µM ^{15}N-complexin-1 in the presence of liposomes containing reconstituted SNARE complex (Figure 3E) suggested that the complexin-1 N-terminus binds to the SNARE complex, which was confirmed by 7-nitrobenz-2-oxa-1,3-diazole fluorescence experiments (Figure 3F; Xue et al., 2010). Mutagenesis supported the physiological relevance of this interaction, leading to a model whereby the complexin-1 N-terminus releases the inhibition caused by the accessory helix and/or stabilizes the C-terminus of the SNARE complex to assist in membrane fusion. A key aspect of this proposal is that, although the interaction of the complexin-1 N-terminus with the SNARE complex C-terminus is weak, it is dramatically favored by the orientation resulting from the tight binding of the central complexin-1 helix to the middle of the SNARE complex (Figure 3G). Although some of the mechanistic details remain to be elucidated, these results provide another example of how interplay between strong and weak interactions can play a critical role in complex molecular mechanisms.

Ca^{2+} sensing by synaptotagmin-1

Since neurotransmitter release was found to be acutely triggered by Ca^{2+} several decades ago, identifying the Ca^{2+} sensor(s) that mediates release became a fundamental question in neuroscience. Synaptotagmin-1 was proposed to be the Ca^{2+} sensor based on the findings that this protein is localized on synaptic vesicles, contains two C$_2$ domains and binds phospholipids in a Ca^{2+}-dependent manner (Perin et al., 1990; Brose et al., 1992). Strong disruption of release was observed in invertebrates lacking synaptotagmin-1, but its role as the Ca^{2+} sensor was questioned because of the persistence of some release in these animals (DiAntonio et al., 1993; Littleton et al., 1993; Nonet et al., 1993). In synaptotagmin-1 KO mice, the major fast component of release was impaired while the asynchronous component was unaffected, suggesting that synaptotagmin-1 acts as the Ca^{2+} sensor for fast release (Geppert et al., 1994).

X-ray crystallography showed that the synaptotagmin-1 C$_2$A domain forms a β-sandwich structure (Sutton et al., 1995), and NMR studies yielded the structures of the Ca^{2+}-bound C$_2$A and C$_2$B domains, showing that they bind three and two Ca^{2+} ions, respectively, through the loops at the top of the β-sandwich (Figure 4A, and Supplementary Figure S2C and D; Shao et al.,

1996, 1998; Ubach et al., 1998; Fernandez et al., 2001). Ca^{2+} binding does not induce substantial conformational changes but causes a dramatic change in the electrostatic potential of the C$_2$ domains that mediates Ca^{2+}-dependent binding to phospholipids, together with insertion of hydrophobic residues into the bilayer (Shao et al., 1997; Chapman and Davis, 1998; Zhang et al., 1998). This knowledge led to the design of point mutations in the C$_2$A domain that decrease or enhance the apparent Ca^{2+} affinity of synaptotagmin-1 and result in parallel changes in the Ca^{2+} sensitivity of neurotransmitter release, providing definitive demonstration that synaptotagmin-1 is the long-sought Ca^{2+} sensor that triggers fast release (Fernandez-Chacon et al., 2001; Rhee et al., 2005).

Mutations in the Ca^{2+} ligands showed that Ca^{2+} binding to the C$_2$B domain is more crucial for release than Ca^{2+} binding to the C$_2$A domain (Fernandez-Chacon et al., 2002; Mackler et al., 2002; Robinson et al., 2002; Nishiki and Augustine, 2004). A likely explanation for these results was provided by DLS and cryo-EM data showing that the C$_2$B domain can bind to two membranes simultaneously (Figure 4B), leading to a model whereby the synaptotagmin-1 C$_2$B domain brings the vesicle and plasma membranes together in a Ca^{2+}-dependent manner, thus cooperating with the SNAREs in triggering fusion (Figure 4C; Arac et al., 2006). This model was supported by the finding that mutations in two arginines in the bottom of the C$_2$B domain (see Figure 4A), which are key for membrane bridging, strongly impair release (Xue et al., 2008).

A crucial question to verify this model and understand the mechanism of release is how the functions of synaptotagmin-1 and the SNAREs are coupled, but confusing results were reported about synaptotagmin-1/SNARE interactions, in part because of the promiscuity of these proteins (Rizo et al., 2006). Moreover, while 1D ^{13}C-edited ^{1}H-NMR spectra of ^{13}C-labeled SNARE complex revealed binding to a synaptotagmin-1 fragment containing its two C$_2$ domains (C$_2$AB fragment), as shown by the decreased signal intensity caused by the C$_2$AB fragment, this decrease was reversed upon addition of liposomes (Figure 4D). This result indicated that the C$_2$AB fragment cannot bind simultaneously to membranes and soluble SNARE complexes, and suggested that SNARE-complex binding might be irrelevant (Arac et al., 2003). However, it was plausible that simultaneous binding could occur with membrane-anchored SNARE complexes, since weak interactions of the membrane-bound C$_2$AB fragment with the SNARE complex might be dramatically enhanced by membrane anchoring of the complex. Indeed, a partition assay using fluorescently labeled C$_2$AB fragment and supported bilayers that contained or lacked reconstituted SNAREs complexes, and that were deposited in separate microchannels, showed a strong preference of the C$_2$AB fragment for the SNARE-complex-containing bilayer (Figure 4E). This finding and additional fluorescence experiments conclusively demonstrated that the C$_2$AB fragment can bind at the same time to the SNARE complex and the lipids (Dai et al., 2007), illustrating the dangers that the divide-and-conquer approach sometimes entails. A structural model of the synaptotagmin-1/SNARE complex assembly built in this study supported the mechanism proposed in Figure 4C, although a single-molecule FRET study led to a different structural model (Choi et al., 2010). Hence,
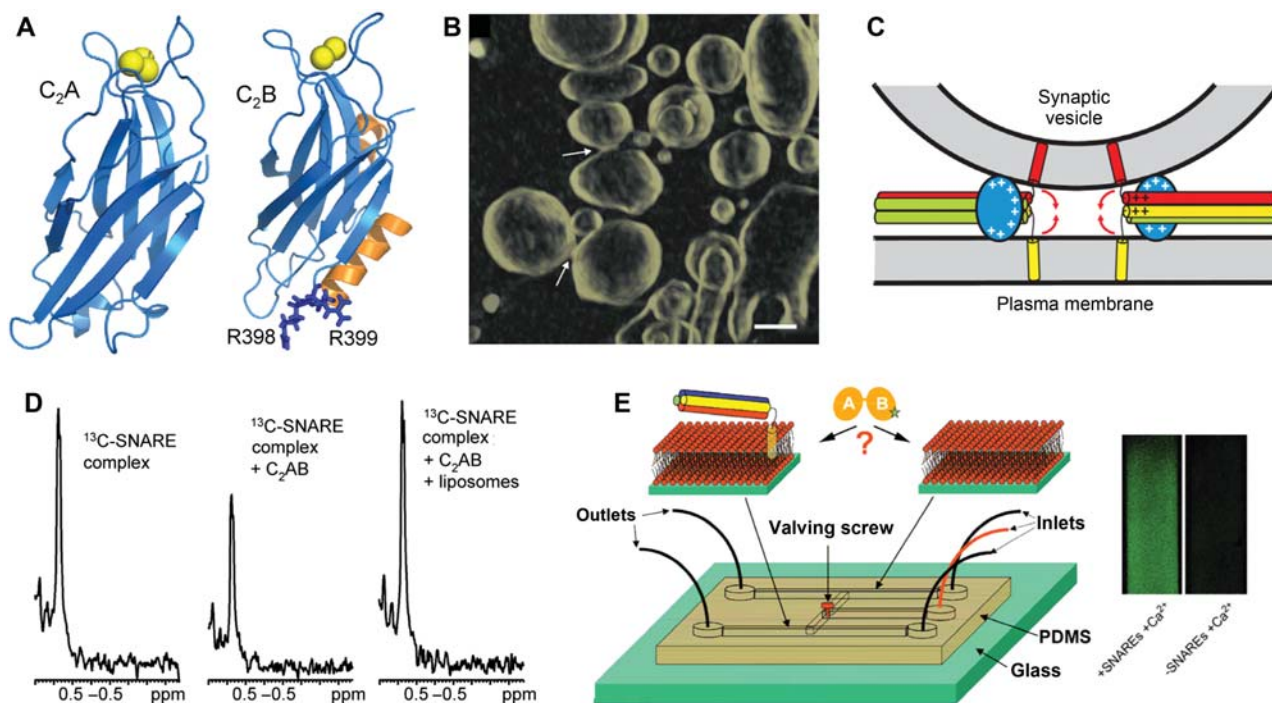
Figure 4 Binding of synaptotagmin-1 to membranes and the SNARE complex. (**A**) Ribbon diagrams of the Ca^{2+}-bound C_2A and C_2B domains of synaptotagmin-1 (Shao et al., 1998; Fernandez et al., 2001). Ca^{2+} ions are shown as yellow spheres. R398 and R399 at the bottom of the C_2B domain are shown as stick models. (**B**) Cryo-EM tomography image of phospholipid vesicles clustered by the synaptotagmin-1 C_2AB fragment. Arrows point to mass density from C_2AB molecules bridging the membranes. Reproduced from Arac et al. (2006). (**C**) Model of how the synaptotagmin-1 C_2B domain (blue) helps to trigger Ca^{2+}-dependent membrane fusion by binding simultaneously to the SNARE complex and the two membranes. Red arrows illustrate that the abundant positive charges of the C_2B domain could help bending the membranes to accelerate fusion (Arac et al., 2006; Xue et al., 2008). (**D**) 1D ^{13}C-edited ^1H-NMR spectra of 1.5 μM ^{13}C-labeled SNARE complex alone or after addition of 2 μM synaptotagmin-1 C_2AB fragment with or without liposomes. Adapted with permission from Arac et al. (2003), copyright (2003) American Chemical Society. (**E**) Experimental setup whereby fluorescently labeled synaptotagmin-1 C_2AB fragment was allowed to partition between plain or SNARE complex-containing supported bilayers deposited into microchannels (left). Confocal images (right) show that the C_2AB fragment partitioned quantitatively to the SNARE complex containing bilayer. Reprinted from Dai et al. (2007), copyright (2007), with permission from Elsevier.

the exact mechanism of synaptotagmin-1 action remains unclear, but both of these studies emphasized the importance of synaptotagmin-1/SNARE interactions and their cooperativity with synaptotagmin-1/membrane binding.

Munc13-1–RIM interactions

In addition to their key function in vesicle priming, Munc13s play multiple roles in presynaptic plasticity processes that underlie multiple forms of information processing in the brain (Rhee et al., 2002; Junge et al., 2004; Shin et al., 2010) and may involve modulation of the priming activity of the MUN domain by other Munc13 domains (Basu et al., 2005, 2007). Among them, the N-terminal C_2A domain of Munc13-1 binds to mammalian RIMs (Betz et al., 2001), which are Rab3 effectors that also play important roles in vesicle priming and presynaptic plasticity (Koushika et al., 2001; Castillo et al., 2002; Schoch et al., 2002; Calakos et al., 2004). Binding to the Munc13-1 C_2A domain is mediated by a zinc finger (ZF) domain within the N-terminal Rab3-binding region of RIMs, and initial pulldown assays suggested that Munc13-1 and Rab3 compete for RIM binding (Betz et al., 2001). However, more robust gel filtration and ^1H-^{15}N

HSQC experiments demonstrated that Munc13-1, RIM and Rab3 actually form a tripartite complex that likely provides a central link between vesicle priming and presynaptic plasticity (Dulubova et al., 2005).

Studies of the Munc13-1-RIM interaction provided another example of the power of combining NMR spectroscopy with X-ray crystallography. The complex between the RIM ZF domain and a Munc13-1 fragment containing the C_2A domain (residues 3–150) exhibited high-quality ^1H-^{15}N HSQC spectra (Figure 5A) but did not yield crystals (Dulubova et al., 2005; Lu et al., 2006). ^1H-^{15}N HSQC spectra of the same Munc13-1 fragment alone were of much lower quality because of aggregation (Figure 5B), but analysis of several Munc13-1 fragments by ^1H-^{15}N HSQC spectra revealed a minimal C_2A domain fragment (residues 3–128) that yielded high quality data (Figure 5C; Lu et al., 2006). All these Munc13-1 fragments form homodimers, as shown by equilibrium sedimentation, but only the minimal fragment yields good NMR spectra because it does not aggregate. Interestingly, the minimal fragment readily yielded high-quality crystals, and elucidation of its crystal structure revealed how the Munc13-1 C_2A domain homodimerizes by forming a β-barrel
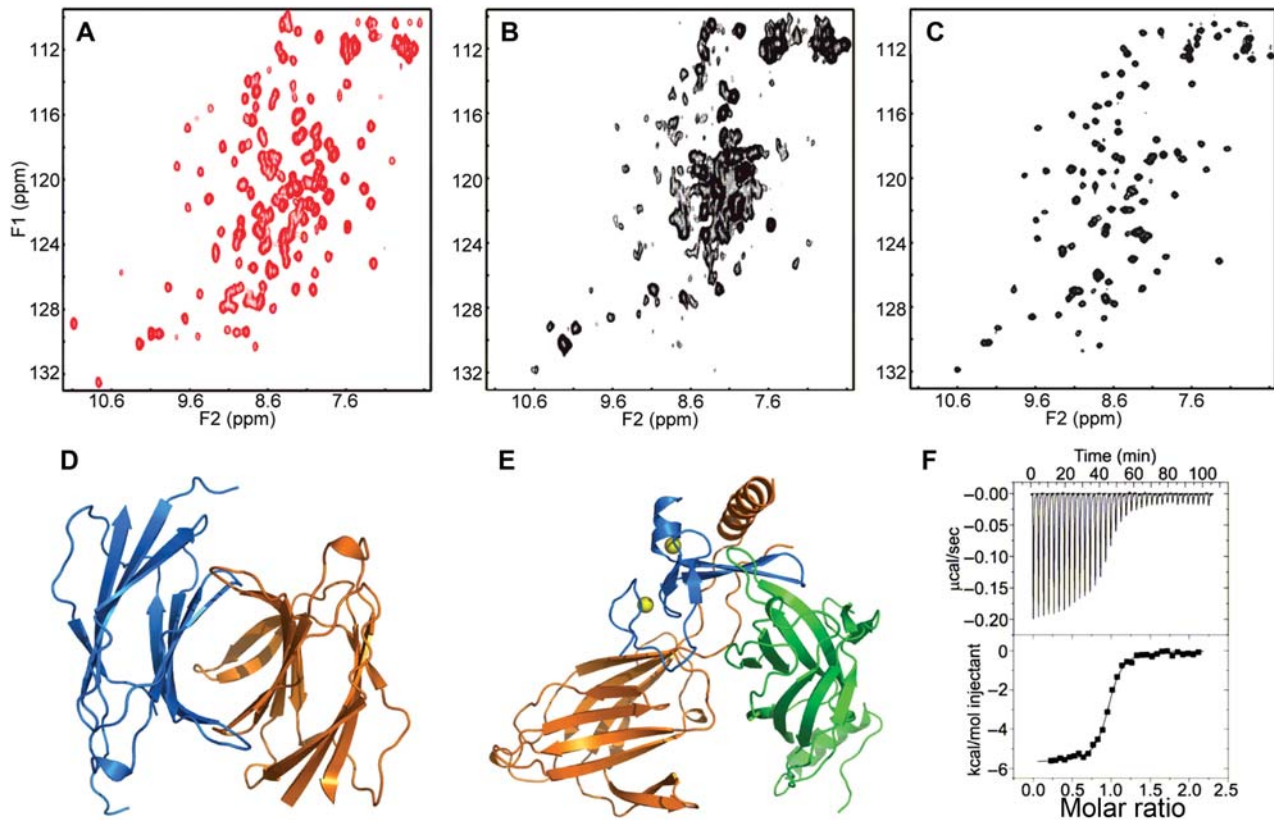
Figure 5 A Munc13-homodimer to Munc13-RIM-heterodimer switch. (**A** and **B**) ^{1}H-^{15}N HSQC spectra of Munc13-1(3−150) bound to the RIM ZF domain (**A**) or alone (**B**). (**C**) ^{1}H-^{15}N HSQC spectrum of Munc13(3−128). (**D** and **E**) Ribbon diagrams of the Munc13-1(3−128) homodimer (**D**) and the RIM ZF-Munc13-1(3−150)K32E heterodimer (**E**) (ZF in blue; two molecules of Munc13-1(3−150)K32E in orange and green). (**F**) ITC analysis of Munc13-1(3−150)K32E/RIM ZF domain binding. All panels reproduced from Lu et al. (2006).

through the concave side of the β-sandwich (Figure 5D). The structure led to the design of a mutation (K32E) that abolishes homodimerization but does not perturb the RIM ZF domain-Munc13-1(3−150) heterodimer (Lu et al., 2006). Importantly, the heterodimer bearing the K32E mutation also yielded high-quality crystals readily, suggesting that the formation of homodimer hindered the crystallization of the WT heterodimer.

Surprisingly, the crystal structure of the RIM ZF domain-Munc13-1(3−150)K32E heterodimer revealed a 1:2 stoichiometry (Figure 5E), even though ^{1}H-^{15}N HSQC spectra (Figure 5A) and ITC (Figure 5F) demonstrated a 1:1 stoichiometry in solution (Lu et al., 2006). One of the two Munc13-1(3−150)K32E molecules in the crystal structure (orange in Figure 5E) wraps around the RIM ZF domain through the C$_2$A domain and a C-terminal α-helical extension, which corresponds to the bona fide binding mode. Conversely, the other Munc13-1(3−150)K32E molecule in the crystals (green in Figure 5E) has much more limited contact with the RIM ZF domain and binding was likely induced by the tendency of the 1:2 complex to crystallize. This structure illustrates that, although crystal structures are normally very reliable, no method is free of potential artifacts. Nevertheless, the crystal structure of the heterodimer still revealed the structural basis for RIM-Munc13-1 binding and allowed the design of a mutation that disrupts the heterodimer and has strong functional effects (Dulubova et al., 2005). Moreover, recent studies showed that

the vesicle priming defects observed in the absence of RIMs can be largely rescued by the RIM ZF domain or by a Munc13 mutant bearing the K32E mutation, but not by WT Munc13 (Deng et al., 2011). Hence, the combination of structural and functional studies has established a clear mechanism whereby homodimerization of Munc13 via the C$_2$A domain inhibits the priming function, and binding of the RIM ZF domain disrupts the homodimer, activating priming by Munc13.

Perspective

The examples discussed above provide just a small glimpse at the vast amount of literature available on the study of molecular mechanisms, but illustrate the power of using diverse biophysical methods to obtain complementary information. The continuous development of powerful NMR techniques suggests that NMR spectroscopy will keep playing an increasingly important role in this area. Particularly promising is the combination of the high sensitivity of ^{1}H-^{13}C HMQC spectra of ^{2}H,^{13}CH$_3$-labeled proteins (Ruschak and Kay, 2010) with measurements of paramagnetic broadening and pseudocontact shifts (Otting, 2010) to study large protein complexes. There are of course continued technical improvements in many other areas of biophysics, including for instance single-molecule fluorescence spectroscopy (Brunger et al., 2009). The future for the study of molecular mechanisms is bright.

Supplementary material

Supplementary material is available at *Journal of Molecular Cell Biology* online.

Conflict of interest: none declared.

References

Arac, D., Murphy, T., and Rizo, J. (2003). Facile detection of protein-protein interactions by one-dimensional NMR spectroscopy. Biochemistry *42*, 2774–2780.

Arac, D., Chen, X., Khant, H.A., et al. (2006). Close membrane-membrane proximity induced by Ca^{2+}-dependent multivalent binding of synaptotagmin-1 to phospholipids. Nat. Struct. Mol. Biol. *13*, 209–217.

Augustin, I., Rosenmund, C., Sudhof, T.C., et al. (1999). Munc13-1 is essential for fusion competence of glutamatergic synaptic vesicles. Nature *400*, 457–461.

Banerjee, A., Barry, V.A., DasGupta, B.R., et al. (1996). N-ethylmaleimide-sensitive factor acts at a prefusion ATP-dependent step in Ca^{2+}-activated exocytosis. J. Biol. Chem. *271*, 20223–20226.

Basu, J., Shen, N., Dulubova, I., et al. (2005). A minimal domain responsible for Munc13 activity. Nat. Struct. Mol. Biol. *12*, 1017–1018.

Basu, J., Betz, A., Brose, N., et al. (2007). Munc13-1 C1 domain activation lowers the energy barrier for synaptic vesicle fusion. J. Neurosci. *27*, 1200–1210.

Bennett, M.K., Calakos, N., and Scheller, R.H. (1992). Syntaxin: a synaptic protein implicated in docking of synaptic vesicles at presynaptic active zones. Science *257*, 255–259.

Betz, A., Thakur, P., Junge, H.J., et al. (2001). Functional interaction of the active zone proteins Munc13-1 and RIM1 in synaptic vesicle priming. Neuron *30*, 183–196.

Bracher, A., and Weissenhorn, W. (2002). Structural basis for the Golgi membrane recruitment of Sly1p by Sed5p. EMBO J. *21*, 6114–6124.

Brewer, K.D., Li, W., Horne, B.E., et al. (2011). Reluctance to membrane binding enables accessibility of the synaptobrevin SNARE motif for SNARE complex formation. Proc. Natl Acad. Sci. USA *108*, 12723–12728.

Brose, N., Petrenko, A.G., Sudhof, T.C., et al. (1992). Synaptotagmin: a calcium sensor on the synaptic vesicle surface. Science *256*, 1021–1025.

Brunger, A.T. (2005). Structure and function of SNARE and SNARE-interacting proteins. Q. Rev. Biophys. *38*, 1–47.

Brunger, A.T., Weninger, K., Bowen, M., et al. (2009). Single-molecule studies of the neuronal SNARE fusion machinery. Annu. Rev. Biochem. *78*, 903–928.

Burkhardt, P., Hattendorf, D.A., Weis, W.I., et al. (2008). Munc18a controls SNARE assembly through its interaction with the syntaxin N-peptide. EMBO J. *27*, 923–933.

Cai, H., Reinisch, K., and Ferro-Novick, S. (2007). Coats, tethers, Rabs, and SNAREs work together to mediate the intracellular destination of a transport vesicle. Dev. Cell *12*, 671–682.

Calakos, N., Bennett, M.K., Peterson, K.E., et al. (1994). Protein-protein interactions contributing to the specificity of intracellular vesicular trafficking. Science *263*, 1146–1149.

Calakos, N., Schoch, S., Sudhof, T.C., et al. (2004). Multiple roles for the active zone protein RIM1 alpha in late stages of neurotransmitter release. Neuron *42*, 889–896.

Carpp, L.N., Ciufo, L.F., Shanks, S.G., et al. (2006). The Sec1p/Munc18 protein Vps45p binds its cognate SNARE proteins via two distinct modes. J. Cell Biol. *173*, 927–936.

Carr, C.M., Grote, E., Munson, M., et al. (1999). Sec1p binds to SNARE complexes and concentrates at sites of secretion. J. Cell Biol. *146*, 333–344.

Castillo, P.E., Schoch, S., Schmitz, F., et al. (2002). RIM1alpha is required for presynaptic long-term potentiation. Nature *415*, 327–330.

Chapman, E.R., and Davis, A.F. (1998). Direct interaction of a Ca^{2+}-binding loop of synaptotagmin with lipid bilayers. J. Biol. Chem. *273*, 13995–14001.

Charbonnier, S., Zanier, K., Masson, M., et al. (2006). Capturing protein-protein complexes at equilibrium: the holdup comparative chromatographic retention assay. Protein Expr. Purif. *50*, 89–101.

Chen, X., Tomchick, D.R., Kovrigin, E., et al. (2002). Three-dimensional structure of the complexin/SNARE complex. Neuron *33*, 397–409.

Choi, U.B., Strop, P., Vrljic, M., et al. (2010). Single-molecule FRET-derived model of the synaptotagmin 1-SNARE fusion complex. Nat. Struct. Mol. Biol. *17*, 318–324.

Dai, H., Shin, O.H., Machius, M., et al. (2004). Structural basis for the evolutionary inactivation of Ca^{2+} binding to synaptotagmin 4. Nat. Struct. Mol. Biol. *11*, 844–849.

Dai, H., Tomchick, D.R., Garcia, J., et al. (2005). Crystal structure of the RIM2 C$_2$A-domain at 1.4 Å resolution. Biochemistry *44*, 13533–13542.

Dai, H., Shen, N., Arac, D., et al. (2007). A quaternary SNARE-synaptotagmin-Ca^{2+}-phospholipid complex in neurotransmitter release. J. Mol. Biol. *367*, 848–863.

Deak, F., Xu, Y., Chang, W.P., et al. (2009). Munc18-1 binding to the neuronal SNARE complex controls synaptic vesicle priming. J. Cell Biol. *184*, 751–764.

Deng, L., Kaeser, P.S., Xu, W., et al. (2011). RIM proteins activate vesicle priming by reversing autoinhibitory homodimerization of Munc13. Neuron *69*, 317–331.

DiAntonio, A., Parfitt, K.D., and Schwarz, T.L. (1993). Synaptic transmission persists in synaptotagmin mutants of Drosophila. Cell *73*, 1281–1290.

Dulubova, I., Sugita, S., Hill, S., et al. (1999). A conformational switch in syntaxin during exocytosis: role of munc18. EMBO J. *18*, 4372–4382.

Dulubova, I., Yamaguchi, T., Wang, Y., et al. (2001). Vam3p structure reveals conserved and divergent properties of syntaxins. Nat. Struct. Biol. *8*, 258–264.

Dulubova, I., Yamaguchi, T., Gao, Y., et al. (2002). How Tlg2p/syntaxin 16 'snares' Vps45. EMBO J. *21*, 3620–3631.

Dulubova, I., Lou, X., Lu, J., et al. (2005). A Munc13/RIM/Rab3 tripartite complex: from priming to plasticity? EMBO J. *24*, 2839–2850.

Dulubova, I., Khvotchev, M., Liu, S., et al. (2007). Munc18-1 binds directly to the neuronal SNARE complex. Proc. Natl Acad. Sci. USA *104*, 2697–2702.

Fasshauer, D., Otto, H., Eliason, W.K., et al. (1997). Structural changes are associated with soluble N-ethylmaleimide-sensitive fusion protein attachment protein receptor complex formation. J. Biol. Chem. *272*, 28036–28041.

Fernandez, I., Ubach, J., Dulubova, I., et al. (1998). Three-dimensional structure of an evolutionarily conserved N-terminal domain of syntaxin 1A. Cell *94*, 841–849.

Fernandez, I., Arac, D., Ubach, J., et al. (2001). Three-dimensional structure of the synaptotagmin 1 C$_2$b-domain. Synaptotagmin 1 as a phospholipid binding machine. Neuron *32*, 1057–1069.

Fernandez-Chacon, R., Konigstorfer, A., Gerber, S.H., et al. (2001). Synaptotagmin I functions as a calcium regulator of release probability. Nature *410*, 41–49.

Fernandez-Chacon, R., Shin, O.H., Konigstorfer, A., et al. (2002). Structure/function analysis of Ca^{2+} binding to the C2A domain of synaptotagmin 1. J. Neurosci. *22*, 8438–8446.

Fiebig, K.M., Rice, L.M., Pollock, E., et al. (1999). Folding intermediates of SNARE complex assembly. Nat. Struct. Biol. *6*, 117–123.

Fletcher, S., Bowden, S.E., and Marrion, N.V. (2003). False interaction of syntaxin 1A with a Ca^{2+}-activated K$^+$ channel revealed by co-immunoprecipitation and pull-down assays: implications for identification of protein-protein interactions. Neuropharmacology *44*, 817–827.

Furgason, M.L., MacDonald, C., Shanks, S.G., et al. (2009). The N-terminal peptide of the syntaxin Tlg2p modulates binding of its closed conformation to Vps45p. Proc. Natl Acad. Sci. USA *106*, 14303–14308.

Garcia, J., Gerber, S.H., Sugita, S., et al. (2004). A conformational switch in the Piccolo C2A domain regulated by alternative splicing. Nat. Struct. Mol. Biol. *11*, 45–53.

Gardner, K.H., and Kay, L.E. (1998). The use of ^{2}H, ^{13}C, ^{15}N multidimensional NMR to study the structure and dynamics of proteins. Annu. Rev. Biophys. Biomol. Struct. *27*, 357–406.

Gelis, I., Bonvin, A.M., Keramisanou, D., et al. (2007). Structural basis for signal-sequence recognition by the translocase motor SecA as determined by NMR. Cell *131*, 756–769.

Geppert, M., Goda, Y., Hammer, R.E., et al. (1994). Synaptotagmin I: a major Ca^{2+} sensor for transmitter release at a central synapse. Cell *79*, 717–727.

Gerber, S.H., Garcia, J., Rizo, J., et al. (2001). An unusual C_2-domain in the active-zone protein piccolo: implications for Ca^{2+} regulation of neurotransmitter release. EMBO J. *20*, 1605–1619.

Gerber, S.H., Rah, J.C., Min, S.W., et al. (2008). Conformational switch of syntaxin-1 controls synaptic vesicle fusion. Science *321*, 1507–1510.

Giraudo, C.G., Garcia-Diaz, A., Eng, W.S., et al. (2009). Alternative zippering as an on-off switch for SNARE-mediated fusion. Science *323*, 512–516.

Guan, R., Dai, H., Tomchick, D.R., et al. (2007). Crystal structure of the RIM1alpha C2B domain at 1.7 Å resolution. Biochemistry *46*, 8988–8998.

Guan, R., Dai, H., and Rizo, J. (2008). Binding of the Munc13-1 MUN domain to membrane-anchored SNARE complexes. Biochemistry *47*, 1474–1481.

Hanson, P.I., Roth, R., Morisaki, H., et al. (1997). Structure and conformational changes in NSF and its membrane receptor complexes visualized by quick-freeze/deep-etch electron microscopy. Cell *90*, 523–535.

Harper, S.M., Neil, L.C., and Gardner, K.H. (2003). Structural basis of a phototropin light switch. Science *301*, 1541–1544.

Hata, Y., Slaughter, C.A., and Sudhof, T.C. (1993). Synaptic vesicle fusion complex contains unc-18 homologue bound to syntaxin. Nature *366*, 347–351.

Hazzard, J., Sudhof, T.C., and Rizo, J. (1999). NMR analysis of the structure of synaptobrevin and of its interaction with syntaxin. J. Biomol. NMR *14*, 203–207.

Huntwork, S., and Littleton, J.T. (2007). A complexin fusion clamp regulates spontaneous neurotransmitter release and synaptic growth. Nat. Neurosci. *10*, 1235–1237.

Jahn, R., and Scheller, R.H. (2006). SNAREs—engines for membrane fusion. Nat. Rev. Mol. Cell Biol. *7*, 631–643.

Junge, H.J., Rhee, J.S., Jahn, O., et al. (2004). Calmodulin and Munc13 form a Ca^{2+} sensor/effector complex that controls short-term synaptic plasticity. Cell *118*, 389–401.

Kaeser, P.S., Deng, L., Wang, Y., et al. (2011). RIM proteins tether Ca^{2+} channels to presynaptic active zones via a direct PDZ-domain interaction. Cell *144*, 282–295.

Khvotchev, M., Dulubova, I., Sun, J., et al. (2007). Dual modes of Munc18-1/SNARE interactions are coupled by functionally critical binding to syntaxin-1 N terminus. J. Neurosci. *27*, 12147–12155.

Kim, A.S., Kakalis, L.T., Abdul-Manan, N., et al. (2000). Autoinhibition and activation mechanisms of the Wiskott-Aldrich syndrome protein. Nature *404*, 151–158.

Koushika, S.P., Richmond, J.E., Hadwiger, G., et al. (2001). A post-docking role for active zone protein Rim. Nat. Neurosci. *4*, 997–1005.

Kreishman-Deitrick, M., Egile, C., Hoyt, D.W., et al. (2003). NMR analysis of methyl groups at 100–500 kDa: model systems and Arp2/3 complex. Biochemistry *42*, 8579–8586.

Kummel, D., Krishnakumar, S.S., Radoff, D.T., et al. (2011). Complexin cross-links prefusion SNAREs into a zigzag array. Nat. Struct. Mol. Biol. *18*, 927–933.

Latham, C.F., Lopez, J.A., Hu, S.H., et al. (2006). Molecular dissection of the Munc18c/syntaxin4 interaction: implications for regulation of membrane trafficking. Traffic *7*, 1408–1419.

Li, W., Ma, C., Guan, R., et al. (2011). The crystal structure of a Munc13 C-terminal module exhibits a remarkable similarity to vesicle tethering factors. Structure *19*, 1443–1455.

Lin, R.C., and Scheller, R.H. (1997). Structural organization of the synaptic exocytosis core complex. Neuron *19*, 1087–1094.

Littleton, J.T., Stern, M., Schulze, K., et al. (1993). Mutational analysis of Drosophila synaptotagmin demonstrates its essential role in Ca^{2+}-activated neurotransmitter release. Cell *74*, 1125–1134.

Lu, J., Machius, M., Dulubova, I., et al. (2006). Structural basis for a Munc13-1 homodimer to Munc13-1/RIM heterodimer switch. PLoS Biol. *4*, e192.

Lu, B., Song, S., and Shin, Y.K. (2010). Accessory alpha-helix of complexin I can displace VAMP2 locally in the complexin-SNARE quaternary complex. J. Mol. Biol. *396*, 602–609.

Ma, C., Li, W., Xu, Y., et al. (2011). Munc13 mediates the transition from the closed syntaxin-Munc18 complex to the SNARE complex. Nat. Struct. Mol. Biol. *18*, 542–549.

Mackler, J.M., Drummond, J.A., Loewen, C.A., et al. (2002). The C_2B Ca^{2+}-binding motif of synaptotagmin is required for synaptic transmission in vivo. Nature *418*, 340–344.

Maximov, A., Tang, J., Yang, X., et al. (2009). Complexin controls the force transfer from SNARE complexes to membranes in fusion. Science *323*, 516–521.

Mayer, A., Wickner, W., and Haas, A. (1996). Sec18p (NSF)-driven release of Sec17p (alpha-SNAP) can precede docking and fusion of yeast vacuoles. Cell *85*, 83–94.

McEwen, J.M., and Kaplan, J.M. (2008). UNC-18 promotes both the anterograde trafficking and synaptic function of syntaxin. Mol. Biol. Cell *19*, 3836–3846.

McMahon, H.T., Missler, M., Li, C., et al. (1995). Complexins: cytosolic proteins that regulate SNAP receptor function. Cell *83*, 111–119.

Misura, K.M., Scheller, R.H., and Weis, W.I. (2000). Three-dimensional structure of the neuronal-Sec1-syntaxin 1a complex. Nature *404*, 355–362.

Nicholson, K.L., Munson, M., Miller, R.B., et al. (1998). Regulation of SNARE complex assembly by an N-terminal domain of the t-SNARE Sso1p. Nat. Struct. Biol. *5*, 793–802.

Nishiki, T., and Augustine, G.J. (2004). Dual roles of the C_2B domain of synaptotagmin I in synchronizing Ca^{2+}-dependent neurotransmitter release. J. Neurosci. *24*, 8542–8550.

Nonet, M.L., Grundahl, K., Meyer, B.J., et al. (1993). Synaptic function is impaired but not eliminated in C. elegans mutants lacking synaptotagmin. Cell *73*, 1291–1305.

Otting, G. (2010). Protein NMR using paramagnetic ions. Annu. Rev. Biophys. *39*, 387–405.

Pabst, S., Hazzard, J.W., Antonin, W., et al. (2000). Selective interaction of complexin with the neuronal SNARE complex. Determination of the binding regions. J. Biol. Chem. *275*, 19808–19818.

Pei, J., Ma, C., Rizo, J., et al. (2009). Remote homology between Munc13 MUN domain and vesicle tethering complexes. J. Mol. Biol. *391*, 509–517.

Perin, M.S., Fried, V.A., Mignery, G.A., et al. (1990). Phospholipid binding by a synaptic vesicle protein homologous to the regulatory region of protein kinase C. Nature *345*, 260–263.

Poirier, M.A., Xiao, W., Macosko, J.C., et al. (1998). The synaptic SNARE complex is a parallel four-stranded helical bundle. Nat. Struct. Biol. *5*, 765–769.

Rathore, S.S., Bend, E.G., Yu, H., et al. (2010). Syntaxin N-terminal peptide motif is an initiation factor for the assembly of the SNARE-Sec1/Munc18 membrane fusion complex. Proc. Natl Acad. Sci. USA *107*, 22399–22406.

Reim, K., Mansour, M., Varoqueaux, F., et al. (2001). Complexins regulate a late step in Ca^{2+}-dependent neurotransmitter release. Cell *104*, 71–81.

Rhee, J.S., Betz, A., Pyott, S., et al. (2002). Beta phorbol ester- and diacylglycerol-induced augmentation of transmitter release is mediated by Munc13s and not by PKCs. Cell *108*, 121–133.

Rhee, J.S., Li, L.Y., Shin, O.H., et al. (2005). Augmenting neurotransmitter release by enhancing the apparent Ca^{2+} affinity of synaptotagmin 1. Proc. Natl Acad. Sci. USA *102*, 18664–18669.

Richmond, J.E., Davis, W.S., and Jorgensen, E.M. (1999). UNC-13 is required for synaptic vesicle fusion in C. elegans. Nat. Neurosci. *2*, 959–964.

Richmond, J.E., Weimer, R.M., and Jorgensen, E.M. (2001). An open form of syntaxin bypasses the requirement for UNC-13 in vesicle priming. Nature *412*, 338–341.

Riek, R., Fiaux, J., Bertelsen, E.B., et al. (2002). Solution NMR techniques for large molecular and supramolecular structures. J. Am. Chem. Soc. *124*, 12144–12153.

Rizo, J., and Sudhof, T.C. (1998). C2-domains, structure and function of a universal Ca^{2+}-binding domain. J. Biol. Chem. *273*, 15879–15882.

Rizo, J., and Rosenmund, C. (2008). Synaptic vesicle fusion. Nat. Struct. Mol. Biol. *15*, 665–674.

Rizo, J., Chen, X., and Arac, D. (2006). Unraveling the mechanisms of synaptotagmin and SNARE function in neurotransmitter release. Trends Cell Biol. *16*, 339–350.

Robinson, I.M., Ranjan, R., and Schwarz, T.L. (2002). Synaptotagmins I and IV promote transmitter release independently of Ca^{2+} binding in the C_2A domain. Nature *418*, 336–340.

Rosen, M.K., Gardner, K.H., Willis, R.C., et al. (1996). Selective methyl group protonation of perdeuterated proteins. J. Mol. Biol. *263*, 627–636.

Ruschak, A.M., and Kay, L.E. (2010). Methyl groups as probes of supramolecular structure, dynamics and function. J. Biomol. NMR *46*, 75–87.

Schoch, S., Castillo, P.E., Jo, T., et al. (2002). RIM1alpha forms a protein scaffold for regulating neurotransmitter release at the active zone. Nature *415*, 321–326.

Shao, X., Davletov, B.A., Sutton, R.B., et al. (1996). Bipartite Ca^{2+}-binding motif in C2 domains of synaptotagmin and protein kinase C. Science *273*, 248–251.

Shao, X., Li, C., Fernandez, I., et al. (1997). Synaptotagmin-syntaxin interaction: the C2 domain as a Ca^{2+}-dependent electrostatic switch. Neuron *18*, 133–142.

Shao, X., Fernandez, I., Sudhof, T.C., et al. (1998). Solution structures of the Ca^{2+}-free and Ca^{2+}-bound C2A domain of synaptotagmin I: does Ca^{2+} induce a conformational change? Biochemistry *37*, 16106–16115.

Shen, J., Tareste, D.C., Paumet, F., et al. (2007). Selective activation of cognate SNAREpins by Sec1/Munc18 proteins. Cell *128*, 183–195.

Shen, J., Rathore, S.S., Khandan, L., et al. (2010). SNARE bundle and syntaxin N-peptide constitute a minimal complement for Munc18-1 activation of membrane fusion. J. Cell Biol. *190*, 55–63.

Shin, O.H., Lu, J., Rhee, J.S., et al. (2010). Munc13 C2B domain—an activity-dependent Ca^{2+} regulator of synaptic exocytosis. Nat. Struct. Mol. Biol. *17*, 280–288.

Sollner, T., Bennett, M.K., Whiteheart, S.W., et al. (1993a). A protein assembly-disassembly pathway in vitro that may correspond to sequential steps of synaptic vesicle docking, activation, and fusion. Cell *75*, 409–418.

Sollner, T., Whiteheart, S.W., Brunner, M., et al. (1993b). SNAP receptors implicated in vesicle targeting and fusion. Nature *362*, 318–324.

Sprangers, R., and Kay, L.E. (2007). Quantitative dynamics and binding studies of the 20S proteasome by NMR. Nature *445*, 618–622.

Stroupe, C., Collins, K.M., Fratti, R.A., et al. (2006). Purification of active HOPS complex reveals its affinities for phosphoinositides and the SNARE Vam7p. EMBO J. *25*, 1579–1589.

Sudhof, T.C. (2004). The synaptic vesicle cycle. Annu. Rev. Neurosci. *27*, 509–547.

Sudhof, T.C., and Rothman, J.E. (2009). Membrane fusion: grappling with SNARE and SM proteins. Science *323*, 474–477.

Sutton, R.B., Davletov, B.A., Berghuis, A.M., et al. (1995). Structure of the first C_2 domain of synaptotagmin I: a novel Ca^{2+}/phospholipid-binding fold. Cell *80*, 929–938.

Sutton, R.B., Fasshauer, D., Jahn, R., et al. (1998). Crystal structure of a SNARE complex involved in synaptic exocytosis at 2.4 Å resolution. Nature *395*, 347–353.

Tang, J., Maximov, A., Shin, O.H., et al. (2006). A complexin/synaptotagmin 1 switch controls fast synaptic vesicle exocytosis. Cell *126*, 1175–1187.

Ubach, J., Zhang, X., Shao, X., et al. (1998). Ca^{2+} binding to synaptotagmin: how many Ca^{2+} ions bind to the tip of a C_2-domain? EMBO J. *17*, 3921–3930.

Ubach, J., Garcia, J., Nittler, M.P., et al. (1999). Structure of the Janus-faced C2B domain of rabphilin. Nat. Cell Biol. *1*, 106–112.

Ubach, J., Lao, Y., Fernandez, I., et al. (2001). The C2B domain of synaptotagmin I is a Ca^{2+}-binding module. Biochemistry *40*, 5854–5860.

Verhage, M., Maia, A.S., Plomp, J.J., et al. (2000). Synaptic assembly of the brain in the absence of neurotransmitter secretion. Science *287*, 864–869.

Weninger, K., Bowen, M.E., Choi, U.B., et al. (2008). Accessory proteins stabilize the acceptor complex for synaptobrevin, the 1:1 syntaxin/SNAP-25 complex. Structure *16*, 308–320.

Xu, Y., Su, L., and Rizo, J. (2010). Binding of Munc18-1 to synaptobrevin and to the SNARE four-helix bundle. Biochemistry *49*, 1568–1576.

Xue, M., Reim, K., Chen, X., et al. (2007). Distinct domains of complexin I differentially regulate neurotransmitter release. Nat. Struct. Mol. Biol. *14*, 949–958.

Xue, M., Ma, C., Craig, T.K., et al. (2008). The Janus-faced nature of the C_2B domain is fundamental for synaptotagmin-1 function. Nat. Struct. Mol. Biol. *15*, 1160–1168.

Xue, M., Craig, T.K., Xu, J., et al. (2010). Binding of the complexin N terminus to the SNARE complex potentiates synaptic-vesicle fusogenicity. Nat. Struct. Mol. Biol. *17*, 568–575.

Yamaguchi, T., Dulubova, I., Min, S.W., et al. (2002). Sly1 binds to Golgi and ER syntaxins via a conserved N-terminal peptide motif. Dev. Cell *2*, 295–305.

Yang, B., Steegmaier, M., Gonzalez, L.C., Jr., et al. (2000). nSec1 binds a closed conformation of syntaxin1A. J. Cell Biol. *148*, 247–252.

Yang, X., Kaeser-Woo, Y.J., Pang, Z.P., et al. (2010). Complexin clamps asynchronous release by blocking a secondary Ca^{2+} sensor via its accessory alpha helix. Neuron *68*, 907–920.

Zhang, X., Rizo, J., and Sudhof, T.C. (1998). Mechanism of phospholipid binding by the C_2A-domain of synaptotagmin I. Biochemistry *37*, 12395–12403.